

**Heavy-fermion characteristics in UCu<sub>5</sub>Al single crystals**

V. H. Tran, R. Troć, J. Stępień-Damm, and T. Komatsubara

*W. Trzebiatowski Institute for Low Temperature and Structure Research, Polish Academy of Sciences, P.O. Box 1410, 50-950 Wrocław, Poland*

F. Steglich

*Max-Planck Institut für Chemische Physik fester Stoffe, D-01187 Dresden, Germany*

R. Hauser and E. Bauer

*Institute of Solid State Physics, T.U. Wien, A-14040 Wien, Austria*

(Received 3 January 2002; revised manuscript received 10 April 2002; published 19 August 2002)

Electronic properties of the antiferromagnetic Kondo compound UCu<sub>5</sub>Al have been investigated through magnetic susceptibility, magnetization, specific heat, electrical resistivity, magnetoresistance, and Hall coefficient measurements on single-crystal and polycrystalline samples. UCu<sub>5</sub>Al orders antiferromagnetically below 16 K and shows a large magnetocrystalline anisotropy. In the paramagnetic state, pronounced incoherent Kondo interactions and crystal field effects are observed. At low temperatures, in spite of the lack of coherence, UCu<sub>5</sub>Al exhibits some characteristic properties of heavy-fermion systems, namely, an enhanced susceptibility, and enhanced electronic specific heat coefficient, revealing an enhanced effective electron mass. The specific heat and transport properties evidence a competition between the Kondo effect and the Ruderman-Kittel-Kasuya-Yosida interactions. This feature, together with the frustration of the magnetic interactions originating from atomic disorder appear to be important for the development of the heavy-fermion state in UCu<sub>5</sub>Al.

DOI: 10.1103/PhysRevB.66.054421

PACS number(s): 75.20.Hr, 71.27.+a

**I. INTRODUCTION**

Heavy-fermion (HF) systems exhibit large values of the electronic specific heat coefficient  $\gamma_0$  and of the magnetic susceptibility  $\chi(0)$  extrapolated to  $T=0$  K, but the so-called Wilson ratio remains constant and is close to 1. In such systems, the effective electron mass is of the order  $(100-300)m_e$ . A characteristic feature of the heavy-fermion behavior is coherence at low temperatures, which manifests itself, among others, by the  $T^2$  behavior of the resistivity. This and other physical properties can be described by the Fermi-liquid formalism. In fact, the enhancement of the effective electron mass is connected to a small Fermi energy, which may appear due to two distinct mechanisms: one is the Abrikosov-Suhl resonance and the other is associated with the occurrence of magnetic correlations; usually such systems are at the edge of a magnetic instability.

Recently, we have investigated the properties of an intermetallic U-based series with the common chemical formula UCu<sub>5</sub>M, where  $M = \text{Al, In, and Sn}$ .<sup>1-3</sup> All these compounds show interesting physical properties, for instance, the Sommerfeld ratio  $C_p/T$  of each of them increases with decreasing temperature, reaching values of the order 200 mJ/K<sup>2</sup> mole U at 1 K. However, the physical properties of these compounds have been studied on polycrystalline samples only. In order to elucidate the observed properties we have undertaken investigations on single-crystalline samples. In this work we will focus on UCu<sub>5</sub>Al. By measuring properties such as the Hall effect and extending the external parameters into high magnetic fields and hydrostatic pressure, a better understanding of this compound is expected.

UCu<sub>5</sub>Al crystallizes in its own structure type with a tetragonal symmetry (space group  $I4/mmm$ ).<sup>4,5</sup> Magnetic sus-

ceptibility, NMR, specific heat, and electrical resistivity measurements<sup>1,6,7</sup> have revealed that antiferromagnetic (AF) order sets in below 18 K. The magnetic structure, determined by neutron powder diffraction scattering, is of a sinusoidally modulated type ( $\vec{k}=0, 0, 0.55$ ) with the amplitude of uranium moments ( $\mu_{\text{ord}}=1.45\mu_B$  at 1.4 K), parallel to the  $c$  axis.<sup>5</sup> Interesting to recall that the Kondo-like behavior of the temperature-dependent electrical resistivity in conjunction with an enhancement of the  $C_p/T$  ratio has classified UCu<sub>5</sub>Al as a medium heavy-fermion system.<sup>7</sup> Very recently, the electronic structure of UCu<sub>5</sub>Al was studied by combining x-ray photoemission spectroscopy results with those of band structure calculations.<sup>8</sup> A complex satellite structure observed in the core level spectra suggests some mixed valence character of the uranium atoms in this ternary compound.

**II. EXPERIMENTAL DETAILS**

Polycrystal samples of UCu<sub>5</sub>Al and U<sub>0.7</sub>Th<sub>0.3</sub>Cu<sub>5</sub>Al were prepared from stoichiometric ratios of starting elements by the standard arc-melting method (see Ref. 1). Single-crystal samples of UCu<sub>5</sub>Al were grown by the Bridgman method. Their orientation and quality were checked by x-ray Laue diffraction. The room temperature lattice parameters of powdered crystals are  $a=6.415(5)$  and  $c=4.946(5)$  Å. These parameters agree well with those previously reported.<sup>5</sup>

Single-crystal x-ray diffraction was performed on a KUMA four-circle diffractometer equipped with CCD camera using graphic-monochromatized MoK $\alpha$  radiation. The intensities of reflections were corrected for Lorentz and polarization effects. The crystal data were refined by the full matrix least-squares method using the SHELX-97 program.<sup>9</sup>

dc magnetization was measured on UCu<sub>5</sub>Al single

crystals by means of a SQUID magnetometer (Quantum Design MPMS-XL) in fields  $H$  up to 50 kOe and in the temperature range 1.7–400 K. The absolute accuracy in  $\chi(T)$  is of about 5%, limited partly by a demagnetizing factor as well as due to a mosaicity of the crystals.

The specific heat measurements  $C_p(T)$ , were performed in a Quantum Design PPMS, utilizing a relaxation method. Data on polycrystalline  $U_{0.7}Th_{0.3}Cu_5Al$  were collected in the temperature range 1.8–100 K and for a  $UCu_5Al$  single crystal in the temperature range 0.4–100 K.

Also the electrical resistivity  $\varrho(T)$  was measured on a  $UCu_5Al$  single crystal along the main crystallographic directions with a Quantum Design PPMS, using a four-probe ac-technique in the temperature range 1.8–300 K. The samples were rectangular with typical dimensions  $0.5 \times 0.5 \times 3$  mm<sup>3</sup>. A current of 5 mA at a frequency of 37 Hz was supplied to the samples. The experimental error in the resistivity is less than 5%, mainly due to the uncertainty in the geometrical factor.

The magnetoresistance (MR) and Hall coefficient  $R_H$  data were collected on  $UCu_5Al$  single crystals in two different ways: isofield data in a fixed magnetic field ( $H = 100$  or  $130$  kOe) on zero-field cooled samples and isothermal data in fields up to 130 kOe at several selected temperatures below 100 K. The magnetic fields were applied perpendicular to the direction of the current.

The magnetoresistance under hydrostatic pressure up to 10 kbar was measured on the polycrystalline  $UCu_5Al$  samples in fields up to 120 kOe at several selected temperatures below 100 K. Hydrostatic pressure was generated by a liquid pressure cell, using a 1:4 ethanol-methanol mixture as the pressure transmitting medium (see, for example, Ref. 10].

### III. RESULTS AND DISCUSSION

#### A. Crystal structure

Previously, based on powder x-ray and neutron diffraction refinements, the crystal structure of  $UCu_5Al$  has been found to have a tetragonal structure with space group  $I4/mmm$ .<sup>5</sup> In this work we have performed the single crystal x-ray refinements on the data collected at room temperature for  $-12 \leq h \leq 12$ ,  $-12 \leq k \leq 8$ , and  $-10 \leq l \leq 6$ . The observed reflections can be fully analyzed by this type of structure and the structure was refined to a reliability factor  $R = 0.03$  for 287 unique reflections and 12 variable parameters. Results of the structural refinements are given in Tables I and II. A listing of the intensity data may be obtained from the authors on request.

From the tables one can recognize that in the unit cell of  $UCu_5Al$  the uranium atoms occupy the twofold position  $2b$  with the coordination polyhedron containing as many as 12 Cu atoms. The four Cu atoms nearest to U are at a distance of 2.804 Å, while the others are at 3.021 Å. This polyhedron does not include the remaining Cu and Al atoms occupying both the same  $4d$  position. The distances between them and the central U atoms are too far (3.439 Å) and these atoms form the next nearest neighbor coordination polyhedron. It is

TABLE I. Crystal data and structure refinement for  $UCu_5Al$ .

Unit cell dimensions (Å)	$a = 6.417(1)$ $c = 4.948(1)$
Calculated density	9.498 mg/m <sup>3</sup>
Absorption coefficient	65.207 mm <sup>-1</sup>
F(000)	500
$\Theta$ range for data collection	4.49° to 46.00°
Reflections collected	1697
Goodness-of-fit	1.101
Final $R$ indices [ $I > 2\sigma(I)$ ]	$R_1 = 0.0287$ , $wR_2 = 0.0601$
$R$ indices (all data)	$R_1 = 0.0291$ , $wR_2 = 0.0603$
Extinction coefficient	0.079(4)
Largest diff. peak and hole	4.089 and -5.252 e.Å <sup>-3</sup>

worth to add that the structure of  $UCu_5Al$  is unique, in the sense that so far there does not exist such a crystal structure for other intermetallics.

#### B. Magnetic properties

The isothermal magnetization of a  $UCu_5Al$  single crystal along the  $a$  and  $c$  axes ( $M_a$  and  $M_c$ ) is shown in Fig. 1(a). At 2 and 10 K the  $M_c(H)$  curve is downward curvilinear, but at temperatures above 20 K the  $M_c(H)$  curves become perfectly proportional to the field. No hysteresis effect in  $M_c(H)$  was observed at any temperature measured. A comparison between  $M_a(H)$  and  $M_c(H)$  reveals a large magnetocrystalline anisotropy.  $M_a(H)$  shows a rather small magnitude; so at 2 K the ratio  $M_c(H)/M_a(H)$  reaches a factor of more than 4, pointing to easy magnetization along the  $c$  axis. For the  $a$ -axis direction the magnetization measured at 2 and 30 K depends linearly on field up to 50 kOe.

In Fig. 1(b), we display the magnetic susceptibility ( $\chi = M/H$ ) measured in the temperature range 1.7–400 K and in two different magnetic fields of 10 and 50 kOe. As can be seen from the  $\chi$  vs  $\ln T$  plot, the magnetocrystalline anisotropy is reflected by a large value of the ratio  $\chi_c/\chi_a$ : At room temperature it amounts to about 2, what is much less than that at the lowest temperature measured at 2 K ( $> 4$ ).

Comparison of the calculated average susceptibility  $\chi_{av} = (2^* \chi_a + \chi_c)/3$  with that of a polycrystalline sample, reveals fairly good agreement with just small preference in the crystalline orientation for the latter. A similar comparison was previously made for an oriented-powder sample.<sup>6</sup> Figure 1(b) evidences that all  $\chi(T)$  curves exhibit a maximum at about  $T_{max}^X = 18$  K. However, according to a theory of

TABLE II. Atomic coordinates, isotropic and anisotropic displacement parameters (Å<sup>2</sup> $\times 10^3$ ) for  $UCu_5Al$ .

	$x$	$y$	$z$	U(eq)	U <sub>11</sub>	U <sub>22</sub>	U <sub>33</sub>
U	0.5000	0.5000	0	7(1)	8(1)	8(1)	6(1)
Cu1	0.1911(1)	0.1911(1)	0	9(1)	9(1)	9(1)	8(1)
Cu2	0.5000	0	0.2500	10(5)	13(6)	13(6)	6(4)
Al	0.5000	0	0.2500	6(10)	6(13)	6(13)	6(13)

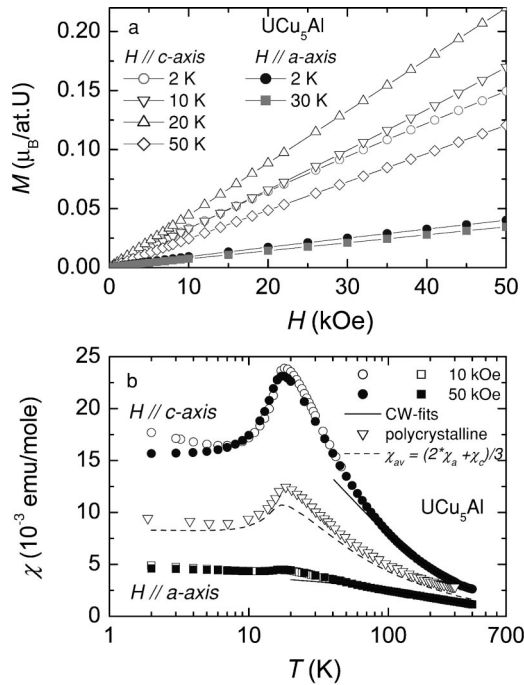


FIG. 1. (a) Isothermal magnetization as a function of magnetic field along the  $a$  and  $c$  axes of a UCu<sub>5</sub>Al single crystal. (b) The temperature dependence of the magnetic susceptibility measured in fields of 10 and 50 kOe along the  $a$  and  $c$  axes of a UCu<sub>5</sub>Al single crystal. Solid lines represent the fits to the Curie-Weiss law. The dashed line represents the calculated susceptibility  $\chi_{av} = (2\chi_a + \chi_c)/3$ . The susceptibility of a polycrystalline sample taken from Ref. 1 (open triangles) is included for comparison.

Fisher,<sup>11</sup> for itinerant antiferromagnets, the Néel temperature is defined as the maximum of the derivative  $d[T\chi(T)]/dT$ . Using this method, we obtain  $T_N = 15.5$  K for UCu<sub>5</sub>Al. This temperature coincides with the characteristic temperatures derived from the specific heat and the electrical resistivity data, as will be evinced in the next subsection.

At temperatures above about 100 K the susceptibility components  $\chi_a(T)$  and  $\chi_c(T)$  can be fitted by the Curie-Weiss (CW) law with the paramagnetic Curie temperature  $\theta_p$  of  $-160$  and  $-46$  K, respectively. Such large negative  $\theta_p$  values, together with the deviations of  $\chi(T)$  from the CW law below 80 K, suggest an influence of the crystal electric field (CEF) and/or the Kondo effect on the magnetic susceptibility. This coincides with the conclusions drawn from the NMR study.<sup>6</sup> The effective magnetic moment of uranium  $\mu_{\text{eff}}$  calculated for the  $a$  and  $c$  axes is  $2.28(5)$  and  $3.02(3)\mu_B/U$ , respectively. Applying Hund's rules, the  $\mu_{\text{eff}}$  values of UCu<sub>5</sub>Al are between the relevant values for the  $5f^1$  ( $\mu_{\text{eff}} = 2.54\mu_B$ ) and  $5f^2$  ( $3.58\mu_B$ ) or  $5f^3$  ( $3.62\mu_B$ ) configurations.

It is interesting to note that rather large susceptibility values are achieved at low temperatures. For example, in a field of 10 kOe, we found  $\chi(0)$  to be  $4.9 \times 10^{-3}$  for the  $a$  axis and  $17.5 \times 10^{-3}$  emu/mole U for the  $c$  axis. These values are comparable to those of other well known heavy-fermion antiferromagnets U<sub>2</sub>Zn<sub>17</sub>,<sup>12</sup> UPd<sub>2</sub>Ga<sub>3</sub>,<sup>13</sup> and UPd<sub>2</sub>Al<sub>3</sub>.<sup>14,15</sup> An interesting feature in  $\chi(T)$  for both the single crystal as well

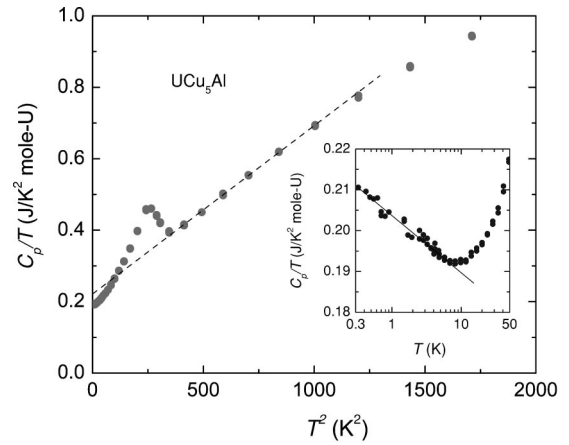


FIG. 2. Specific heat divided by temperature vs squared temperature for a UCu<sub>5</sub>Al single crystal. The dashed line indicates the  $(\gamma_p + \beta T^2)$  dependence of  $C_p/T$ . The inset shows the  $C_p/T$  vs  $\log T$  down to 0.4 K. The solid line is a guide for the eyes.

as the polycrystalline sample is a minimum around 9 K, below which  $\chi(T)$  increases. Usually this type of behavior is ascribed in the literature to a paramagnetic impurity. Here, however, we consider such a behavior being intrinsic. This is because the susceptibility measured in various magnetic fields is distinctly suppressed for the  $c$  axis, but only a very weak change was observed for the  $a$  axis in fields as high as 50 kOe. It seems unlikely that an impurity effect is also anisotropic. In addition, the  $\chi_c$  data at temperatures below 5 K could not be described by a CW law, which hardly supports any effect of paramagnetic impurity. We think that the low-temperature  $\chi(T)$  behavior of UCu<sub>5</sub>Al is connected with the presence of substantial magnetic fluctuations at low temperatures. Bearing in mind the fact that the sine-modulated magnetic structure of UCu<sub>5</sub>Al reflects frustration in the exchange interactions, and hence may become unstable when the temperature is lowered. Of course if the system has not a nonmagnetic ground state then it starts to show a tendency, for instance, for squaring up. As a consequence, the crossover into a new magnetic state may give rise to the magnetic susceptibility increase. However, as the specific heat data indicate, which are given in the next subsection, at least down to 0.4 K there is no evidence for such a crossover. Another possibility of the low-temperature  $\chi$  upturn can be that the system becomes strongly correlated with magnetic moments being suppressed by the Kondo interactions. For example, within the multichannel Kondo model, the low-field magnetization is expected to follow a power-law field dependence.<sup>16-18</sup> Therefore, the resulting susceptibility diverges logarithmically. In fact, for UCu<sub>5</sub>Al, the low-temperature data of  $\chi_c(T)$  can be well fitted by an expression  $\chi_c(T) = \chi(0) + a \ln T$ , with  $\chi(0) = 18.5 \times 10^{-3}$  emu/mole U and  $a = -1.2 \times 10^{-3}$  emu/K mole U.

### C. Specific heat

In Fig. 2, we show the temperature dependence of the specific heat  $C_p$  as  $C_p/T$  vs  $T^2$  for a UCu<sub>5</sub>Al single crystal. Clearly there is a somewhat diffuse maximum in  $C_p(T)/T$  at

$T = 15.8$  K which agrees well with that found in polycrystalline sample specific heat measurements,<sup>1</sup> and concurs with  $T_N$  deduced from the susceptibility measurements. We recognize that if there is no transition below 0.4 K, the electronic coefficient  $\gamma_0 = C_p/T(T \rightarrow 0)$  reaches a value as large as  $\sim 210(5)$  mJ/K<sup>2</sup> mole U (see the inset of Fig. 2). An even larger value of  $C_p/T$  (about 220 mJ/K<sup>2</sup> mole U) is found by extrapolating the data measured above  $T_N$  to  $T = 0$ . The latter value may represent the electronic specific heat coefficient in the paramagnetic state  $\gamma_p$ . In any case, there is an enhancement in both  $\gamma_p$  and  $\gamma_0$  values, indicating a development of a heavy-fermion state in UCu<sub>5</sub>Al (for comparison, the  $\gamma_p$  value for UPd<sub>2</sub>Al<sub>3</sub> is 140 mJ/K<sup>2</sup> mole U<sup>14</sup>). Similar to several AF HF materials (U<sub>2</sub>Zn<sub>17</sub>, UCd<sub>11</sub>, UNi<sub>2</sub>Al<sub>3</sub>, etc.)  $\gamma_p > \gamma_0$ . This finding strongly suggests a pseudogapping in the Fermi-surface associated with the AF ordering.

For a number of heavy-fermion materials the expression of the Wilson ratio

$$R_W = \frac{\chi(0)}{3\gamma} \left( \frac{\pi k_B}{\mu_{\text{eff}}} \right)^2 \quad (1)$$

can be used to distinguish between the contributions to the total susceptibility caused by magnetic fluctuations and that due to the Abrikosov–Suhl resonance arising from the Kondo effect. Taking  $\gamma_p = 220$  mJ/K<sup>2</sup> mole U and the average values of  $\chi_{\text{av}}(0)$  and  $(\mu_{\text{eff}})_{\text{av}}$  we estimated for UCu<sub>5</sub>Al  $R_W = 1.3$ . This number is between those reported for UPd<sub>2</sub>Al<sub>3</sub> (0.7) (Ref. 14) and UPd<sub>2</sub>Ga<sub>3</sub> (2.1),<sup>13</sup> indicating the importance of magnetic fluctuations taking place at low temperatures in UCu<sub>5</sub>Al.

In order to quantify the  $C_p(T)$  data of UCu<sub>5</sub>Al, the phonon contribution has to be defined. This task, however, is not easy since no nonmagnetic homologous compound with the same structure has so far been recognized. Because isostructural U<sub>0.7</sub>Th<sub>0.3</sub>Cu<sub>5</sub>Al is nonmagnetic down to 2 K,<sup>1</sup> we can assume that the total specific heat of this phase consists of two contributions only; i.e., the electronic ( $C_{\text{el}}$ ) and phonon part ( $C_{\text{ph}}$ ) origin. It is obvious from the inset of Fig. 3 that  $C_{\text{el}}/T = \gamma_p = 82$  mJ/K<sup>2</sup> mole derived from a high-temperature extrapolation can be separated from the total specific heat by plotting the data as  $C_p(T)/T$  vs  $T^2$ . An inspection of the crystal structure of U<sub>0.7</sub>Th<sub>0.3</sub>Cu<sub>5</sub>Al, suggests two different Einstein frequencies for the U and Th atoms, respectively. Therefore, an analysis of the lattice specific heat  $C_{\text{ph}}$ , should take into consideration three main contributions, one expressed as a Debye and two as Einstein terms:

$$C_{\text{ph}}(T) = 9Rn_D \left( \frac{T}{\Theta_D} \right)^3 \int_0^{\Theta_D/T} \frac{x^4 \exp(x)}{(\exp(x) - 1)^2} dx + 3R \sum \frac{n_{E_i} (\Theta_{E_i}/T)^2 \exp(\Theta_{E_i}/T)}{[\exp(\Theta_{E_i}/T) - 1]^2}, \quad (2)$$

where  $n_D = 6$  and  $n_E = 0.7$  and 0.3 are the numbers of the Debye and Einstein oscillators, respectively. After separating the electronic contribution from the total specific heat, we have fitted the Eq. (2) to the data. All the contributions to  $C_p$

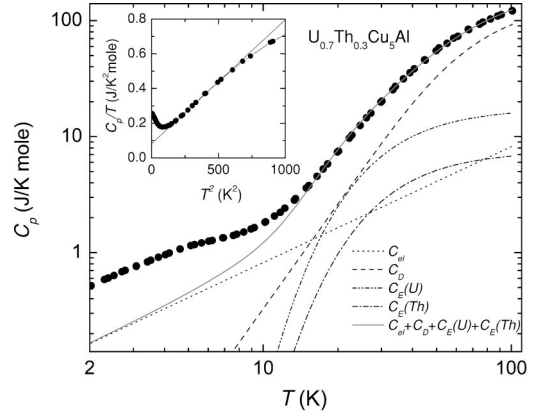


FIG. 3. Temperature dependence of the specific heat of nonmagnetic U<sub>0.7</sub>Th<sub>0.3</sub>Cu<sub>5</sub>Al. The fit and its four contributions: an electronic ( $C_{\text{el}}$ ), a Debye ( $C_D$ ), and two Einstein ( $C_E(U)$  and  $C_E(\text{Th})$ ) ones, are shown as lines specified in the figure. The solid line gives a sum of all the contributions. The inset shows the low-temperature specific heat as  $C_p/T$  vs  $T^2$ . The solid line is a fit of  $C_p/T = \gamma + \beta T^2$  to the experimental data.

are shown in Fig. 3 as a  $C_p$  vs  $\ln T$ . We obtain  $\Theta_D = 329$  K,  $\Theta_E(U) = 106$  K, and  $\Theta_E(\text{Th}) = 108$  K. When subtracting the approximate lattice contribution [ $\Theta_D = 329$  K,  $\Theta_E(U) = 106$  K] from the total specific heat of UCu<sub>5</sub>Al, the 5f-electron contribution is derived. The results of this analysis are given in Fig. 4 as  $C_{5f}/T$  vs  $T$ .

For temperatures between 4–14 K, the magnetic specific heat  $C_{5f}$  follows the dependence predicted by the spin-wave theory for antiferromagnetic system<sup>19–21</sup>

$$C_{5f}(T) = \gamma_0 T + BT^3 \exp(-\Delta/T). \quad (3)$$

The parameters  $\gamma_0$  and  $B$  denote the coefficient of the electronic specific heat in the AF state and the contribution of antiferromagnetic magnons, respectively. The exponential factor on the right-hand side of Eq. (3) indicates a gap  $\Delta$  in the magnon excitation spectrum of UCu<sub>5</sub>Al below  $T_N$ . A

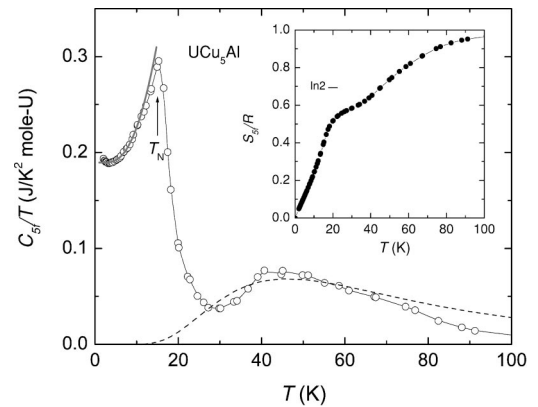


FIG. 4. The magnetic part of the specific heat divided by temperature  $C_{5f}/T$  as a function of temperature. The thick solid and dashed lines represent the best fit in terms of the spin-wave and Schottky theory, respectively (see the text for details). The solid line is the guide for eyes. The magnetic entropy normalized to  $R$ ,  $S_{5f}/R$ , as a function of temperature is shown in the inset.

best fit to the data yields  $\gamma_0 = 189(2)$  mJ/K<sup>2</sup>mole U,  $B = 1.31(1)$  mJ/K<sup>4</sup> mole U, and  $\Delta = 13(1)$  K.

Below  $\sim 4$  K,  $C_p/T$  no longer follows Eq. (3), since there is an anomalous upturn with decreasing temperature (see inset, Fig. 2). At present, there is no explanation for this upturn, but a similar behavior with  $C_p(T)/T \sim -T^2 \ln T$ , reflecting magnetic fluctuations or NFL states at low temperatures, has already been reported for a number of HF compounds.<sup>17,22</sup>

Roughly around 45 K, a maximum occurs in  $C_{5f}(T)/T$  which is ascribed to a Schottky anomaly. For a two-level systems, the Schottky specific heat is written as

$$C_{\text{Sch}}(T) = R \left( \frac{\Delta E}{T} \right)^2 \frac{g_0}{g_1} \frac{\exp(\Delta E/T)}{[1 + (g_0/g_1) \exp(\Delta E/T)]^2}. \quad (4)$$

The best fit of the Schottky contribution gives a crystal-field ground state and an excited state of equal degeneracies ( $g_0/g_1 = 1$ ) with an energy splitting  $\Delta E = 150$  K.

The inset of Fig. 4 shows the magnetic entropy  $S_{5f}$ , calculated by an integration of  $\int_0^{100 \text{ K}} [C_{5f}(T)/T] dT$ . It is interesting to note that the magnetic entropy release at  $T_N$  of UCu<sub>5</sub>Al is only about 64% the value expected for a doublet ground state  $R \ln 2$ . Similar reduced values of the magnetic entropy were found, e.g., in UPd<sub>2</sub>Al<sub>3</sub>,<sup>23</sup> for which  $S_{5f}$  amounts only to  $\sim 35\%$   $R \ln 2$  at  $T_N$ . Usually, the reduction in the magnetic entropy below that expected for a doublet ground state at transition temperature is interpreted in terms of either an itinerant electron magnetism of magnetic ions or as being caused by the Kondo screening effect. However, one should bear in mind that the unambiguous separation of the phonon part from the total heat capacity is difficult.

#### D. Electrical transport properties

In Fig. 5(a), we compare the temperature dependent normalized electrical resistivity  $\rho/\rho(300 \text{ K})$  of the configuration  $j//c$  axis with that of  $j//a$  axis. The arrow included in the figure indicates the Néel temperature estimated from the susceptibility and specific heat data. As can be seen, there is nice agreement between the magnetic, specific heat, and electrical resistivity data; the latter exhibit a distinct change in its slope. A dominant feature is the large anisotropy which appears in the entire temperature range measured. For  $j//c$  axis, the resistivity  $\rho(T)$  shows a maximum at  $T_{\text{max}}^{\rho} = 40$  K, followed by a significant decrease just below  $T_N$  due to the onset of the AF order. At lower temperatures, the resistivity conforms approximately a  $T^2$  dependence. Therefore, the overall resistivity behavior for  $j//c$  bears a resemblance to that of a Kondo-lattice compounds and within the scope of theory developed by Fischer,<sup>24</sup>  $T_{\text{max}}^{\rho}$  might be ascribed to the freezing-out of incoherent Kondo scattering.

If we try to fit the low-temperature  $\rho$  data for  $j//c$  with

$$\rho(T) = \rho_0 + aT^2 + bT(1 + 2T/\Delta) \exp(-\Delta/T) \quad (5)$$

used previously, e.g., in UPd<sub>2</sub>Al<sub>3</sub> (Ref. 25) and URu<sub>2</sub>Si<sub>2</sub> (Ref. 26) we get  $\rho_0 = 173.5 \mu\Omega \text{ cm}$ ,  $a = 0.08(1) \mu\Omega \text{ cm/K}^2$  and  $b = 0.25(2) \mu\Omega \text{ cm/K}$ . The energy gap  $\Delta = 13$  K was

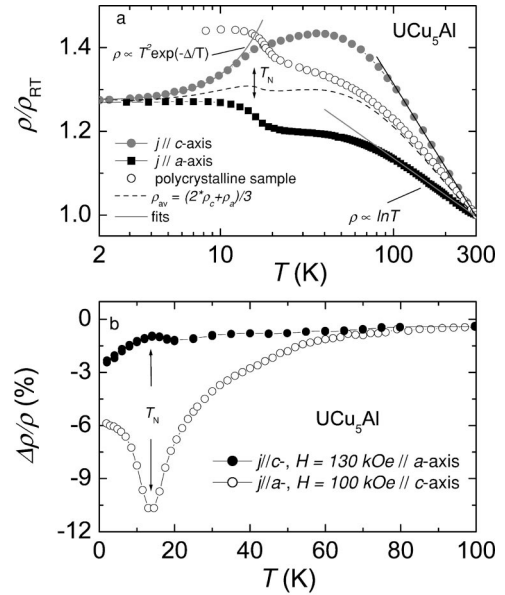


FIG. 5. (a) Temperature dependence of the resistivity in zero field of a UCu<sub>5</sub>Al single crystal measured with current along the  $a$  and  $c$  axes. The solid lines are the fits according to Eqs. (5) or (6). Dashed line represents the average resistivity  $\rho_{\text{av}} = (2\rho_c + \rho_a)/3$ . For a comparison the resistivity of a polycrystalline sample (open circles) is also included. (b) The temperature dependence of the magnetoresistance  $(\Delta\rho/\rho)_i = [\rho_i(H, T) - \rho_i(0, T)] * 100/\rho_i(0, T)$  of a UCu<sub>5</sub>Al single crystal ( $i = a$  or  $c$ ).

used from the specific heat measurements. It should be noted that the above equation was first used by Andersen and Smith<sup>27</sup> for describing the electron-magnon interaction in Tb. The meanings of the coefficients are as follows:  $\rho_0$  is the residual resistivity, the  $T^2$  term represents Fermi-liquid behavior and  $b$  denotes the electron-magnon coupling.

In contrast to the low-temperature  $\rho_c(T)$  behavior,  $\rho_a(T)$  for  $j//a$ , before saturate at very low temperatures, a steplike increase occurs in the vicinity of  $T_N$ , probably due to the formation of a gap in the spin-wave spectrum caused by the formation of the incommensurate structure in UCu<sub>5</sub>Al. The absolute value of  $\rho_a$  is large, and for instance, at 2 K it amounts to  $\sim 445 \mu\Omega \text{ cm}$  compared to  $173 \mu\Omega \text{ cm}$  for the  $c$  axis. It is somewhat surprising because the overall  $\rho_a$  resistivity of the single crystal sample is remarkably larger than the value obtained for the polycrystalline sample. At 4 K it amounts to  $\sim 175 \mu\Omega \text{ cm}$ .<sup>1</sup> However, it is well known that the observed  $\rho$  value of such a sample is combined from various contributions and often it shows a distinct preference to one of the axes. Nevertheless, for a sake of clarity we also present the average resistivity  $\rho_{\text{av}} = (2\rho_c + \rho_a)/3$  as a dashed line in Fig. 5(a). This enables one to make a comparison with the previously reported data on a polycrystalline sample. We recognize, however, that the relative temperature change of the resistivity of UCu<sub>5</sub>Al is rather small. This feature is certainly caused by atomic disorder introduced by a random distribution of Cu<sub>II</sub> and Al on the ( $4d$ ) site of the unit cell.<sup>5</sup> Furthermore, we observe a fairly good agreement between  $\rho_{\text{av}}$  and the resistivity of the polycrystalline sample for  $T$

>100 K. In this temperature range all the resistivities of UCu<sub>5</sub>Al measured above follow the expression

$$\rho(T)/\rho(300 \text{ K}) \propto c \ln T \quad (6)$$

describing incoherent Kondo scattering. It is also clear from Fig. 5(a) that the coefficient  $c$  for  $j//c$  is more negative than at for  $j//a$  or for the polycrystalline sample. The observed data for  $j//c$  are striking because the measurements performed on the polycrystalline sample of UCu<sub>5</sub>Al and the solid solutions (U<sub>1-x</sub>Th<sub>x</sub>)Cu<sub>5</sub>Al,<sup>1</sup> as well as on a single crystal along  $j//a$  did not show any signature of coherence; only a tendency to saturation is observed for  $T \rightarrow 0$  K.

The influence of magnetic fields on the resistivity is shown in Fig. 5(b). The temperatures of the maximum in the magnetoresistance  $\Delta\rho(T)/\rho$  for  $j//c$  and the minimum in  $\Delta\rho(T)/\rho$  for  $j//a$  track the  $T_N$  value. We deal here with a suppression of the antiferromagnetic transition temperature by magnetic field, e.g.,  $H$  of 130 kOe shifts  $T_N$  down to 13 K. As is also seen from Fig. 5(b), an applied magnetic field  $H$  reduces  $\rho(T)$  for both directions, resulting in a negative magnetoresistance. In fact, a large change in the MR magnitude is observed for  $j//a$ , reaching about  $-11\%$  at  $T_N$ . In the case of the polycrystalline sample the reduction in the resistivity was even larger, leading to the MR at  $T_N$  of about 27%.<sup>7</sup> Below  $T_N$ , however, the MR increases, showing that the positive MR associated with an antiferromagnetic order starts to overcome the Kondo interactions. Above  $T_N$  the large negative magnitude of MR for this configuration decreases and vanishes roughly at  $2T_N$ . The MR for  $j//c$  behaves in a different manner; it shows some negative maximum at  $T_N$  probably connected with the incommensurate magnetic structure with moments directed parallel to the  $c$  axis.

In order to examine in more detail the influence of the Kondo effect on the MR, we performed such measurements for several temperatures and in fields up to 130 kOe. Figure 6(a) shows the data obtained for  $j//a$ . One sees that the largest MR values are observed for isotherms in the vicinity of  $T_N$ . This finding is consistent with the interpretation of the formation of a small gap in the AF state, which simply becomes suppressed by the applied magnetic field. It is noted that the shape of isothermal MR curves for  $T > T_N$  is qualitatively similar for one another and resembles that observed in a single-ion Kondo system. Schlottmann<sup>28</sup> has shown that the MR in the Kondo impurity systems can be calculated by applying the Bethe *ansatz* technique to the Copblin-Schrieffer Hamiltonian. His model predicts a negative MR which exhibits a universal behavior as a function of the applied field. It means that the Kondo properties can be accounted for by a single energy scale  $g_J\mu H^*$ , which is related to the relation<sup>29</sup>

$$H^*(T) = H^*(0) + \frac{k_B}{g_J\mu_K} T = \frac{k_B}{g_J\mu_K} (T_K + T), \quad (7)$$

where  $\mu_K$  stands for the Kondo-screened magnetic moment and  $T_K$  is the Kondo temperature. Other symbols have usual meaning. In spite of the fact that this model has already been

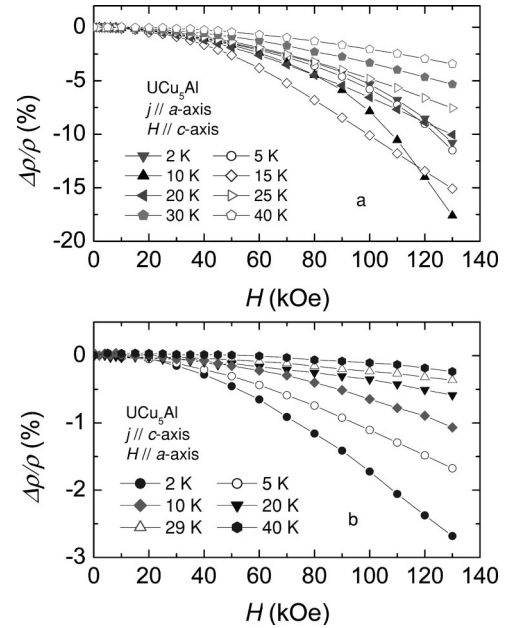


FIG. 6. Isothermal magnetoresistance as a function of an applied field of a UCu<sub>5</sub>Al single crystal with (a) the current along the  $a$  axis and the field along the  $c$  axis and (b) the current along the  $c$  axis and the field along the  $a$  axis.

applied to a few other uranium-based Kondo systems, such as UBe<sub>13</sub> (Ref. 30) and U<sub>x</sub>Th<sub>1-x</sub>Pd<sub>2</sub>Al<sub>3</sub>,<sup>31</sup> it is not clear to us whether the obtained  $T_K$  value has any significance. Therefore, instead of  $T_K$  we signify the characteristic energy scale by  $T^*$ , assuming that  $T^*$  is proportional to  $T_K$ . Applying the Schlottmann model to the MR data of the UCu<sub>5</sub>Al single crystal, we get rather small values for this characteristic temperature, namely  $T^* = 3 \pm 0.5$  K for  $j//a$ . A similar field dependence is also observed for the MR measured along  $j//c$  [Fig. 6(b)]. For the latter, we derived also a small value of  $T^* = 2 \pm 0.5$  K, though a large difference in the MR values for the two directions exists.

We have also analyzed the MR data obtained for the polycrystalline sample of UCu<sub>5</sub>Al under pressure on the basis of the Schlottmann model mentioned above. For illustration, we show in Fig. 7 such a fit for the MR data under  $P = 3.1$  kbar by the solid lines. In the inset of this figure, the temperature dependence of the characteristic field  $H^*$ , as deduced from the fits, is shown. The linear behavior of  $H^*$  vs  $T$  for  $T > T_N$  yields  $T^*$  about 9 K for  $P = 3.1$  kbar (see the inset). In the same manner, the MR data obtained for  $P = 6$  and 10 kbar were analyzed, yielding,  $T^* = 22(2)$  and 19(3) K, respectively. These results indicate that applied pressure causes an increase of the Kondo temperature. An interesting observation we have made is that pressure shifts the temperature of the MR maximum to lower temperature (Fig. 8); this leads to the fact that  $T_N$  under  $P = 10$  kbar ( $\sim 8.6$  K) is considerably lower than that under ambient pressure, roughly by a factor of 2. This is further illustrated in the inset of Fig. 8 with a plot of  $T_{\max}$  as a function of the pressure. A qualitative understanding of the pressure response in UCu<sub>5</sub>Al can be revealed from the Kondo-lattice model of Doniach,<sup>32</sup> in

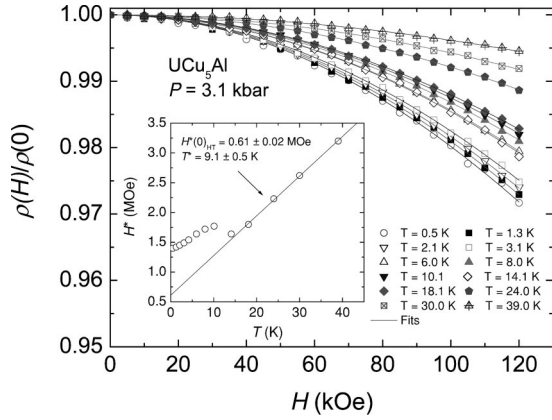


FIG. 7. Isothermal magnetoresistance (MR) as a function of the field of polycrystalline UCu<sub>5</sub>Al under pressure of 3.1 kbar. The inset shows the temperature dependence of the characteristic field  $H^*$ , as deduced from the fits (see text).

which the Kondo and RKKY interactions compete with each other under pressure. The positive effect of pressure on  $T_K$  and the negative one on  $T_N$  implies for UCu<sub>5</sub>Al:  $T_K \gtrsim T_{\text{RKKY}}$ .

Figure 9 shows the temperature dependence of the Hall coefficient  $R_H$  for  $H//a$  and  $H//c$ . The Hall coefficient is highly anisotropic with much larger value for  $H//c$ . For both directions,  $R_H$  shows a positive value and increases with decreasing temperature. Around 20 K,  $R_H$  for  $H//c$  exhibits a hump, and a tail with further decreasing temperature, while for  $H//a$  a local maximum with a small tail at the lowest temperatures is found. The occurrence of this maximum at temperature higher than  $T_N$  suggests that coherent scattering from the uranium sublattice starts to develop. In the scope of the theory of the Hall effect for HF compounds,<sup>33</sup> the position of this maximum can be taken as a measure of the coherence temperature  $T_{\text{coh}}$ . However, the development of coherence is interrupted by the antiferromagnetic phase transition at 15.8 K. Below this temperature, owing to the opening of spin-wave gap the Hall coefficient increases

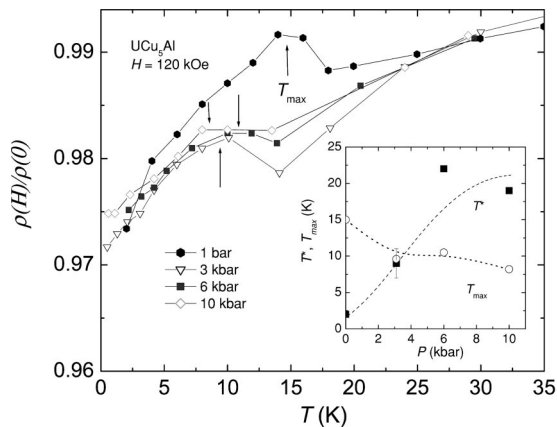


FIG. 8. The temperature dependence of the magnetoresistance  $\rho(H)/\rho(0)$  of UCu<sub>5</sub>Al in 120 kOe and under pressure 3, 6, and 10 kbar. The inset shows the temperature dependence of  $T_{\text{max}}$  and  $T^*$ .

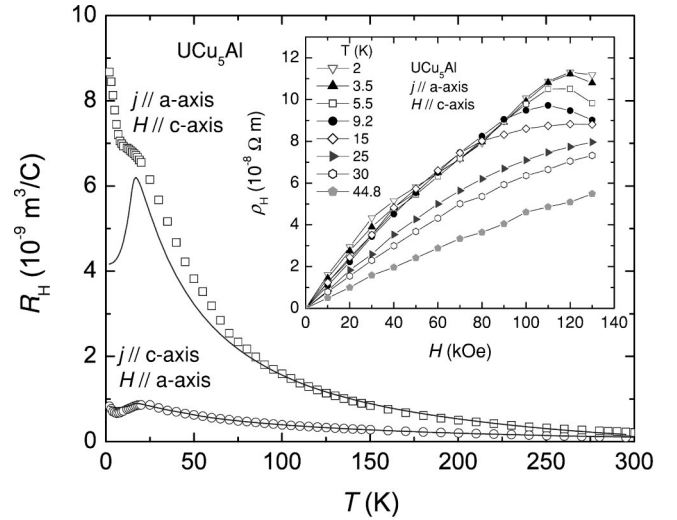


FIG. 9. Temperature dependence of the Hall coefficient  $R_H$  for a UCu<sub>5</sub>Al single crystal. The solid lines are the calculated dependencies based on the skew scattering theory. The inset shows the isothermal Hall resistivity for  $j//a$  and  $H//c$  axes.

sharply with further decreasing temperature. A similar behavior has been observed in HF antiferromagnets such as U<sub>2</sub>Zn<sub>17</sub> (Ref. 34) and URu<sub>2</sub>Si<sub>2</sub>.<sup>35</sup>

For  $T \gg T_K$ , the skew scattering gives rise to a peak in the temperature dependence of the Hall coefficient. It means that, in addition to the temperature-independent ordinary scattering term  $R_0$ , the Hall coefficient also contains a skew scattering term  $R_{\text{sk}}$ . For many HF systems, the Hall coefficient in the incoherent state follows roughly the dependence

$$R_H = R_0 + R_{\text{sk}} = R_0 + \gamma_1 \tilde{\chi} \rho_m, \quad (8)$$

where  $\rho_m$  is the magnetic resistivity and  $\tilde{\chi} = \chi/C$  ( $C$  is the Curie constant). The coefficient  $\gamma_1$ , related to the phase shift  $\delta_2$ , takes a form

$$\gamma_1 = -\frac{5}{7} g \mu_B k_B^{-1} \sin \delta_2 \cos \delta_2. \quad (9)$$

Assuming that the contribution due to electron-phonon scattering to the resistivity below 300 K is negligible, we could fit the experimental data to Eq. (8) with  $R_0 = -1.245 \times 10^{-10} \text{ m}^3/\text{C}$  and  $\gamma_1 = 7.827 \times 10^{-2} \text{ K/T}$  for  $H//a$  and  $R_0 = -6.438 \times 10^{-10} \text{ m}^3/\text{C}$  and  $\gamma_1 = 7.877 \times 10^{-2} \text{ K/T}$  for  $H//c$ . The results of such a fit are shown in Fig. 9 as solid lines. This indicates that the incoherent skew scattering by the U-5*f* moments dominates the temperature dependence of the Hall coefficient at temperatures above  $T_N$ . The minus sign of  $R_0$  indicates that electrons predominate the ordinary Hall coefficient.

An interesting comparison can be made with the data of other HF systems. The sign of  $\gamma_1$  for UCu<sub>5</sub>Al is found to be positive, which is characteristic for HF systems.<sup>33,36,37</sup> It is worth noting that the values of  $\gamma_1$  are almost the same for both measured configurations, corresponding to a phase shift of the partial wave  $\delta_2$  by about  $-24^\circ$ . From the  $R_0$  values,

we obtain within a one-band model, carrier densities  $n = 5.0 \times 10^{28} \text{ m}^{-3}$  ( $-4.9$  carriers/f.u.) and  $9.7 \times 10^{27} \text{ m}^{-3}$  ( $-0.9$  carrier/f.u.) for  $H//a$  and  $H//c$ , respectively. Taking into account the  $\gamma$  value from our specific heat results, we can estimate the effective electron mass of  $\text{UCu}_5\text{Al}$ . Taking  $\gamma_0 = 210 \text{ mJ/K}^2 \text{ mole U}$  and the values of carrier density  $n$ , we estimate  $m^* = 55$  and  $105 m_e$  for  $H//a$  and  $H//c$  axes, respectively. These are in values typical for medium heavy-electron systems.

Inset of Fig. 9 shows the isothermal Hall resistivity ( $\rho_H$ ) of  $\text{UCu}_5\text{Al}$  for the configuration  $j//a$  axis. A transition from the antiferromagnetic state to the paramagnetic one can be deduced from these plots. Below  $T_N$  two important pictures are observed: the initial slope  $d\rho_H/dH$  reaches a maximum value at  $T=2 \text{ K}$ , and  $\rho_H$  shows a hump at  $H$  around 30–40 kOe being next followed by another maximum at  $\sim 120 \text{ kOe}$ . One perceives that the position of these anomalies shifts to lower fields with increasing temperature. This behavior can be interpreted as a suppression of magnetic scattering connected with a spin-flop Kondo process. In the paramagnetic temperature range,  $\rho_H$  is strongly nonlinear in magnetic field. Such a behavior is expected, if the Hall resistivity is dominated by the skew scattering.<sup>33</sup>

#### IV. CONCLUSION

The experimental data on  $\text{UCu}_5\text{Al}$  single crystals demonstrate that the magnetic and transport properties of this compound are strongly anisotropic. In the paramagnetic state these properties are governed by both the anisotropic Kondo and crystalline electric field effects, while below  $T_N$  they are caused by the competition between the Kondo effect and the RKKY interactions. This competition results in a frustrated magnetic state, such as an incommensurate structure which largely influences the thermodynamic properties of  $\text{UCu}_5\text{Al}$ . Furthermore,  $\text{UCu}_5\text{Al}$  shows some characteristic properties of a HF antiferromagnet, such as the localized magnetic moment at high temperatures and an enhanced effective electron mass at low temperatures. However, the underlying physics seems to be more complicated than that applied previously for other classical HF compounds. First of all, it is well known in a number of HF compounds that the Kondo compensation yields not only an enhanced density of states at the Fermi energy driving the system to the formation of heavy quasiparticles, and simultaneously screens the local moments. Despite that the neutron scattering experiments cannot exclude the presence, e.g., of a spin-density wave, involving itinerant  $5f$  electrons, the amplitude of the magnetic moment is as large as  $1.5\mu_B/\text{U}$  at 1.5 K. For  $\text{UCu}_5\text{Al}$  it is possible that the effect of Kondo compensation may be not as strong as in the other nonmagnetic HF systems, because the Kondo effect usually becomes quenched by the magnetic order. Instead, we found some evidences for the itinerant

nature of the magnetic moments: the low entropy at  $T_N$  and a large value of the electronic coefficient of the specific heat. This feature is much supported by the electronic structure calculations and XPS experiments.<sup>8</sup> On the other hand, an antiferromagnetism with relative large ordered moments ( $\sim 0.85\mu_B/\text{U}$ ) was previously observed for a few HF compounds such as  $\text{U}_2\text{Zn}_{17}$  (Ref. 38) and  $\text{UPd}_2\text{Al}_3$ .<sup>39</sup> In the latter compound, the existence of two independent  $5f$ -subsystems has been proposed to explain the coexistence of the HF superconductivity and magnetic order.<sup>40,41</sup> In this model, it was assumed the presence of the subsystem with a small mass enhancement is responsible for the local moment antiferromagnetism, and the other subsystem being more itinerant determining the heavy-fermion characteristics of this compound. Perhaps, such a two-subsystem picture is also valid for  $\text{UCu}_5\text{Al}$ , and further experiments such as the pressure dependence of the specific heat or the inelastic neutron scattering should give a more correct description in the future.

The occurrence of the upturn in both  $C_p/T$  and the magnetic susceptibility at low temperatures is an interesting feature, but within the single-ion Kondo model one cannot describe the observed phenomenon. It is obvious that these observations differ somewhat from those which can be expected from the Fermi-liquid behavior. Although there are many theoretical approaches to the non-Fermi-liquid behavior; one of them which may be useful to describe the observed here an increase in the  $C_p/T$  and  $\chi$  at low temperatures is a multichannel Kondo effect.<sup>16,18</sup> However, one should remember that  $\text{UCu}_5\text{Al}$ , with an intrinsic atomic disorder in the unit cell, can be an origin of the magnetic moment frustration. As a consequence of it, the magnetic moments at different atomic sites become nonequivalent and just such a situation starts to dominate the thermodynamic and transport properties of  $\text{UCu}_5\text{Al}$ . Crystallographic disorder may lead to a distribution of Kondo temperatures.<sup>42,43</sup> For example, this model has been used to explain the non-Fermi-liquid behavior in the disordered  $\text{UCu}_{5-x}\text{Pd}_x$  system.<sup>44,45</sup>

In summary, we have presented the magnetic, thermodynamic and electron transport properties for  $\text{UCu}_5\text{Al}$ . The experimental data indicate that the development of the heavy-fermion state in this compound is more complicated than that described previously for other HF systems. Magnetic fluctuations seem to be important and need further microscopic investigations, notably of the  $^{63}\text{Cu}$  NMR spin lattice relaxation rate  $1/T_1$ .

#### ACKNOWLEDGMENTS

The work at INT&BS PAN Wrocław was supported by the State Committee for Scientific Research in Poland within Grant No. 2P03B 150 17. Parts of the work were supported by the Austrian FWF, Grant No. 12899.

- <sup>1</sup>R. Troć, R. Andruszkiewicz, R. Pietri, and B. Andraka, *J. Magn. Magn. Mater.* **183**, 132 (1998).
- <sup>2</sup>V. H. Tran, R. Troć, R. Pietri, and B. Andraka, *Phys. Rev. B* **60**, 4696 (1999).
- <sup>3</sup>D. Kaczorowski, R. Troć, A. Czopnik, A. Jeżowski, Z. Henkie, and V. I. Zaremba, *Phys. Rev. B* **63**, 144401 (2001).
- <sup>4</sup>C. Geibel, S. Thies, D. Kaczorowski, C. Schank, A. Mehner, B. Seidel, and F. Steglich (unpublished).
- <sup>5</sup>R. Troć, V. H. Tran, M. Wołczyrz, C. André, and F. Bourée, *J. Magn. Magn. Mater.* **190**, 251 (1998).
- <sup>6</sup>B. Nowak and R. Troć, *Solid State Nucl. Magn. Reson.* **14**, 157 (1999).
- <sup>7</sup>R. Troć, V. H. Tran, D. Kaczorowski, and A. Czopnik, *Acta Phys. Pol. A* **97**, 25 (2000).
- <sup>8</sup>G. Chełkowska, J. A. Morkowski, A. Szajek, and R. Troć, *Phys. Rev. B* **64**, 075119 (2001).
- <sup>9</sup>G. M. Sheldrick, SHELX-97, Program for Crystal Structure Refinement, University of Göttingen, Germany, 1997.
- <sup>10</sup>R. Hauser, E. Bauer, and E. Gratz, *Phys. Rev. B* **57**, 2904 (1998).
- <sup>11</sup>M. E. Fisher, *Philos. Mag.* **7**, 1731 (1962).
- <sup>12</sup>H. R. Ott, H. Rudigier, P. Delsing, and Z. Fisk, *Phys. Rev. Lett.* **52**, 1551 (1984).
- <sup>13</sup>S. Süllow, B. Ludoph, B. Becker, G. J. Nieuwenhuys, A. A. Menovsky, J. A. Mydosh, S. A. M. Mentink, and T. E. Mason, *Phys. Rev. B* **52**, 12 784 (1995).
- <sup>14</sup>C. Geibel, C. Schank, S. Thies, H. Kitazawa, C. D. Bredl, A. Böhm, M. Rau, A. Grauel, R. Caspary, R. Helfrich, U. Ahlheim, G. Weber, and F. Steglich, *Z. Phys. B: Condens. Matter* **84**, 1 (1991).
- <sup>15</sup>N. Sato, N. Aso, N. Tateiwa, N. Koga, T. Komatsubara, and N. Metoki, *Physica B* **230-232**, 367 (1997).
- <sup>16</sup>P. Schlottmann and P. D. Sacramento, *Adv. Phys.* **42**, 641 (1993).
- <sup>17</sup>See, for example, *J. Phys.: Condens. Matter* **8**, 48 (1996).
- <sup>18</sup>D. L. Cox and A. Zawadowski, *Adv. Phys.* **47**, 599 (1998).
- <sup>19</sup>O. V. Lounasmaa and L. J. Sundström, *Phys. Rev.* **150**, 399 (1966).
- <sup>20</sup>N. Tateiwa, N. Sato, and T. Komatsubara, *Phys. Rev. B* **58**, 11 131 (1998).
- <sup>21</sup>N. Andrei, K. Furuya, and J. H. Lowenstein, *Rev. Mod. Phys.* **55**, 331 (1983).
- <sup>22</sup>F. J. Ohkawa, *Phys. Rev. B* **44**, 6812 (1991).
- <sup>23</sup>I. H. Hagemus, J. C. P. Klaasse, E. Brück, A. A. Menovsky, and F. R. de Boer, *Physica B* **246&247**, 464 (1998).
- <sup>24</sup>K. H. Fischer, *Z. Phys. B: Condens. Matter* **74**, 475 (1989).
- <sup>25</sup>Y. Dalichaouch, M. C. de Andrade, and M. B. Maple, *Phys. Rev. B* **46**, 8671 (1992).
- <sup>26</sup>H. Ohkuni, Y. Inada, Y. Tokiwa, K. Sakurai, R. Settai, T. Honma, Y. Haga, E. Yamamoto, Y. Onuki, H. Yamagami, S. Takahashi, and T. Yamagisawa, *Philos. Mag. B* **79**, 1045 (1999).
- <sup>27</sup>N. H. Andersen and H. Smith, *Phys. Rev. B* **19**, 384 (1979).
- <sup>28</sup>P. Schlottmann, *Z. Phys. B: Condens. Matter* **51**, 223 (1983).
- <sup>29</sup>B. Batlogg, D. J. Bishop, E. Bucher, B. Golding, A. P. Ramirez, Z. Fisk, J. L. Smith, and H. R. Ott, *J. Magn. Magn. Mater.* **63&64**, 441 (1987).
- <sup>30</sup>U. Rauchschwalbe, F. Steglich, and H. Rietschel, *Physica B* **148**, 33 (1987).
- <sup>31</sup>P. de V du Plessis, A. M. Strydom, R. Troć, T. Cichorek, Cz. Marucha, and R. P. Gers, *J. Phys.: Condens. Matter* **11**, 9775 (1999).
- <sup>32</sup>S. Doniach, *Physica B* **91**, 231 (1997).
- <sup>33</sup>A. Fert and P. M. Levy, *Phys. Rev. B* **36**, 1907 (1987).
- <sup>34</sup>T. Siegrist, M. Olivier, S. P. McAlister, and R. W. Cochrane, *Phys. Rev. B* **33**, 4370 (1986).
- <sup>35</sup>J. Schoenes, C. Schönenberger, J. J. M. Franse, and A. A. Menovsky, *Phys. Rev. B* **35**, 5375 (1987).
- <sup>36</sup>A. Hamzic and A. Fert, *J. Magn. Magn. Mater.* **76&77**, 221 (1988).
- <sup>37</sup>R. Köhler, H. Fischer, C. Schank, C. Geibel, F. Steglich, N. Sato, and T. Komatsubara, *Physica B* **206&207**, 430 (1995).
- <sup>38</sup>D. E. Cox, G. Shirane, S. M. Shapiro, G. Aeppli, Z. Fisk, J. L. Smith, J. Kjems, and H. R. Ott, *Phys. Rev. B* **33**, 3614 (1986).
- <sup>39</sup>A. Krimmel, P. Fischer, B. Roessli, M. Maletta, C. Geibel, C. Schank, A. Grauel, A. Loidl, and F. Steglich, *Z. Phys. B: Condens. Matter* **86**, 161 (1992).
- <sup>40</sup>R. Caspary, P. Hellmann, M. Keller, G. Sparn, C. Wassilew, R. Köhler, C. Geibel, C. Schank, F. Steglich, and N. E. Phillips, *Phys. Rev. Lett.* **71**, 2146 (1993).
- <sup>41</sup>N. K. Sato, N. Aso, K. Miyake, R. Shiina, P. Thalmeier, G. Varelogiannis, C. Geibel, F. Steglich, P. Fulde, and T. Komatsubara, *Nature (London)* **410**, 340 (2001).
- <sup>42</sup>O. O. Bernal, D. E. MacLaughlin, H. G. Lukefahr, and B. Andraka, *Phys. Rev. Lett.* **75**, 2023 (1995).
- <sup>43</sup>E. Miranda, V. Dobrosavljevic, and G. Kotliar, *J. Phys.: Condens. Matter* **8**, 9871 (1996); *Phys. Rev. Lett.* **78**, 290 (1997).
- <sup>44</sup>B. Andraka and G. R. Stewart, *Phys. Rev. B* **47**, 3208 (1993).
- <sup>45</sup>R. Chau and M. B. Maple, *J. Phys.: Condens. Matter* **8**, 9939 (1996).